FTIR and FT-Raman spectra and density functional computations of the vibrational spectra, molecular geometry and atomic charges of the biomolecule: 5-Bromouracil

ARTICLE *in* JOURNAL OF RAMAN SPECTROSCOPY · OCTOBER 2007

Impact Factor: 2.67 · DOI: 10.1002/jrs.1725

7 AUTHORS, INCLUDING:

Vijay Rastogi
Easton Hospital Easton PA 18045
96 PUBLICATIONS **981** CITATIONS
SEE PROFILE

Mauricio Alcolea Palafox
Complutense University of Madrid
129 PUBLICATIONS **1,436** CITATIONS
SEE PROFILE

Niculina Peica
Thermo Fisher Scientific
29 PUBLICATIONS **245** CITATIONS
SEE PROFILE

Wolfgang Kiefer
University of Wuerzburg
878 PUBLICATIONS **9,847** CITATIONS
SEE PROFILE

JOURNAL OF RAMAN SPECTROSCOPY
J. Raman Spectrosc. 2007; **38**: 1227–1241
Published online 22 August 2007 in Wiley InterScience
(www.interscience.wiley.com) DOI: 10.1002/jrs.1725

JRS

FTIR and FT-Raman spectra and density functional computations of the vibrational spectra, molecular geometry and atomic charges of the biomolecule: 5-bromouracil

V. K. Rastogi,[1]* M. A. Palafox,[2] L. Mittal,[3] N. Peica,[4] W. Kiefer,[4] K. Lang[5] and S. P. Ojha[1]

[1] Department of Physics, CCS University, Meerut-250 004, India
[2] Departmento of Quimica-Fisica (Espectroscopia), Facultad de Ciencias Quimicas, Universidad Compultense, Madrid-28040, Spain
[3] Department of Physics, Inderprastha Engineering College, Ghaziabad-201010, India
[4] Institut für Physikalische Chemie, Universität Würzburg, Am Hubland, D-97074 Würzburg, Germany
[5] Department of Kinetics, Institute of Inorganic Chemistry, Academy of Sciences of Czech Republic

Received 12 October 2006; Accepted 4 January 2007

FTIR and FT-Raman spectra of 5-bromouracil in the powder form were recorded in the region 400–4000 cm^{-1} and 50–4000 cm^{-1}, respectively. The observed wavenumbers were analysed and assigned to different normal modes of vibration of the molecule. Quantum chemical calculations were performed to support the assignments of the observed wavenumbers. The performance of the B3LYP hybrid density functional (DFT) method was compared with other methods. With the 6–31 G** and 6–311+G(2d,p) basis sets, the calculated geometry, dipole moments and harmonic vibrations were determined. A comparison with the uracil molecule was made, and specific scale factors were deduced and employed in the predicted wavenumbers of 5-bromouracil. The total atomic charges and thermodynamic parameters were calculated, and are discussed briefly. Structure and harmonic vibrations of 5-bromouracil were also calculated in the presence of water within a simple model with one molecule. It is observed that the bromine atom at position 5 exhibits smaller inductive effects than the fluorine atom, producing a small distortion of the electrostatic potential around the ring and a reduction of the molecular dipole moment.

KEYWORDS: FTIR and FT-Raman spectra; density functional computations; molecular geometry; atomic charges; biomolecule; 5-bromouracil

INTRODUCTION

The halogenated pyrimidines were synthesised in the 1950s as potential anti-tumour agents after the discovery that certain tumours preferentially incorporated uracil rather than thymine into the DNA.[1] Among these compounds the 5-halogenated uracils deserve special attention. Transformation of uracil into 5-X uracil (X = halogen) significantly changes its chemical and spectroscopic properties, as well as its *in vivo* activity. They have been found to exert profound effects in a variety of microbiological and mammalian systems. It has been suggested that 5-halogeno derivatives may adopt rare hydroxy forms more easily than the non-substituted uracil and therefore can act as a stronger mutagenic agent. Extensive work, both theoretical and experimental, have been done on uracil and its derivatives.[2–5] 5-Chlorouracil and 5-bromouracil (5-BrU) have been studied to treat inflammatory tissues.[6,7] The 5- and 6-halouracils have also been investigated as a possible class of radio-sensitisers, which are used to control damage to healthy tissues in radiation therapy.[8] However, their vibrational spectra have not been completely and accurately interpreted. This task can be satisfactorily carried out with the use of density functional theory (DFT). As a first step towards this study of 5-halogenated pyrimidines, we have studied the vibrational spectra of 5-fluorouracil: an anticancer drug.[3] This compound is widely recognised today as an effective treatment modality, especially with tumours of the head, neck and breast.[1,4] DNA normally contains uncommon nucleotides usually in very small amount. 5-Bromouracil is one of the well-known uncommon nucleotide bases and has the ability

*Correspondence to: V. K. Rastogi, Department of Physics, CCS University, Meerut-250 004, India.
E-mail: v_krastogi@rediffmail.com

to co-ordinate metals or to bind to tissues via metals. In order to extend this study further, the present work has been undertaken on 5-bromouracil, which also interfaces with the growth of cancer cells.

Substitution of thymine with 5-BrU in DNA is known to change interaction between DNA and proteins (increase the cross-linking efficiency and reduce the direct damage), thereby inducing various biological phenomena.[9,10] These DNA-interacting sites have been identified.[11,12] Several studies reveal its great medicinal importance.[3,13] 5-BrU forms complexes with MS2 RNA-protein.[14] Incorporated into nuclear DNA, 5-BrU is a well-known mutagen,[15] and repairs the replication of damaged DNA in UV irradiated bacteria.[16] In contrast to DNA, the presence of 5-BrU in DNA-PNA (peptide nucleic acid) chimeras destabilised the triple helix.[17] Mixed-ligand complexes of Co(II), Ni(II), Cu(II), Zn(II) and Cd(II) with adenine as primary ligand and 5-BrU as secondary ligand have been reported.[18–22] Oligonucleotides containing 5-BrU have been used to study the radiation-induced electron migration (a mechanism that randomly can lead to a damage along DNA) in nucleic acids.[23–25]

From spectroscopy point of view, 5-BrU in the gas phase has been studied by several experimental techniques, such as dissociative electron attachment (DEA),[26] electronic absorption and fluorescence emission spectra,[27,28] NMR[29,30] and ESR.[31] Its vibrational spectra have been also studied without any theoretical support: the Raman spectra by Rai,[32] and the FTIR in an Ar-matrix by Graindourze *et al*.,[33,34] Gusakova *et al*.,[35] Srivastava *et al*.[36] and Sanyal *et al*.[37] However, there are doubts in the assignment of several bands because the compound is highly fluorescent in nature.[38,39] In our previous work, IR and Raman studies on this molecule have also been reported, but again without theoretical support.[40] During the process of preparation of the present paper, a good report on the Ar-matrix IR spectra of 5-halouracils has also been published.[41] However, the present work on 5-BrU remarkably improves upon the earlier results, identifying all the bands for the first time and reviewing the assignments of several bands. Hartree-Fock (HF) and density functional *ab initio* calculations were performed to support our wavenumber assignments. To the best of our knowledge, such studies have not been reported earlier on 5-BrU.

The specific interactions between the purine and pyrimidine bases are one of the corner stones of molecular biology. These interactions, which underlie the transmission of genetic information, are governed in large part by the NH···O or NH···N hydrogen bonds, and they are expected to depend not only on the proton acceptor ability of the O or N atoms but also on the intrinsic acidity of the NH bonds involved in the interaction. As first step in this study and to shed more light on the accurate prediction of geometry and spectroscopic characteristics of the molecule in question in the gas phase and in water, detailed MO calculations can be compared with the earlier reported data of uracil.[42] The hydration of 5-halo derivatives have been reported only in 5-FU.[43,44]

EXPERIMENTAL

5-Bromouracil (solid state) of spectral grade was purchased from M/s Aldrich Chemical Co (Milwankee, WI, USA) and used as such without any further purification.

The FT-Raman spectrum of 5-BrU was recorded at room temperature in the powder form in the region 50–4000 cm^{-1} on a Bruker IFS66 optical bench with an FRA 106 Raman module attachment. The sample was mounted on the sample illuminator using an optical mount and no sample pretreatment was undertaken. The NIR output (1064 nm) of an Nd:YAG laser was used to excite (the probe) the spectrum. The instrument was equipped with a liquid-nitrogen-cooled Ge detector. The laser power was set at 100 mW and the spectrum was recorded over 1000 scans at a fixed temperature. The spectral resolution was 6.0 cm^{-1} after apodisation.

The mid-infrared spectrum of the compound from 400–4000 cm^{-1} was recorded with a Perkin Elmer FTIR model 1760 X instrument, using the KBr technique with 1 mg sample per 300 mg KBr. For the spectrum acquisition, four scans were collected at 4 cm^{-1} resolution.

COMPUTATIONAL METHODS

Ab initio calculations[45] with wavefunction-based HF and MP2,[46] and DFT[47] were used. The DFT hybrid methods with the Becke exchange functional (B)[48] and the Becke's three-parameter exchange functional (B3),[49,50] and in combination with the correlational functional of Lee, Yang and Parr (LYP),[51] Perdew 1986 (P86),[52,53] Perdew and Wang's 1991 (PW91),[54,55] and modified Perdew-Wang 91 (MPW1PW91)[56] were used. These hybrid functionals were selected for their better predicting ability of the molecular properties. The basis sets used in this work are the two standard ones widely used for quantum chemical studies because of their reasonable quality and size: 6–31G** and 6–311+G(2d,p). Dunning's correlation-consistent basis sets double (cc-pVDZ) and triple-zeta (cc-pVTZ) have also been used.[57–59] The presence of both polarization and diffuse functions in the basis set is necessary for a proper theoretical description of the molecular parameters. These procedures are implemented in the Gaussian 98 program package,[60] which was utilized in the Unix version with standard parameters.

The optimum geometry was determined, with the keyword OPT, by minimising the energy with respect to all geometrial parameters without imposing molecular symmetry constraints. Berny optimization under the tight convergence criteria was used. Harmonic wavenumbers were calculated to characterise the stationary points and to evaluate the wavenumber shifts due to complex formation

DOI: 10.1002/jrs

with water. The keyword Freq = Raman was used for this task and at the same level of the respective optimisation process. The keyword Raman was employed to obtain Raman values. All the optimised structures showed positive harmonic vibrations only (true energy minimum). For the calculation of the zero-point vibrational energy (ZPE), the wavenumbers were retained unscaled.

RESULTS AND DISCUSSIONS

Geometry optimisation

Non-hydrated form

The optimised bond lengths and angles for 5-BrU using *ab initio* and DFT methods are given in Table 1, while the labelling of the atoms is plotted in Fig. 1. For comparison purposes, in the last three columns of Table 1 are collected the experimental data reported by X-ray and by electron diffraction (ED) in the uracil molecule,[61–63] together with their calculated values by B3LYP.

When the bromine atom is introduced in the position 5 of the uracil molecule, a small effect is observed in the molecular structure, e.g. the calculated C═C and C–C═bond lengths at B3LYP/6-31G** level in 5-BrU, 1.3513 Å and 1.4699 Å, respectively, appear very close to those determined in uracil molecule, 1.3498 Å and 1.4602 Å, respectively. The other bond lengths are observed to change insignificantly. The angles C–C5═C and O═C4═N3 in 5-BrU are found to be 120.37° and 120.87°, respectively, which are fairly close to the corresponding values of 119.94° and 120.38° in uracil. However, large errors were determined[3] in 5-FU.

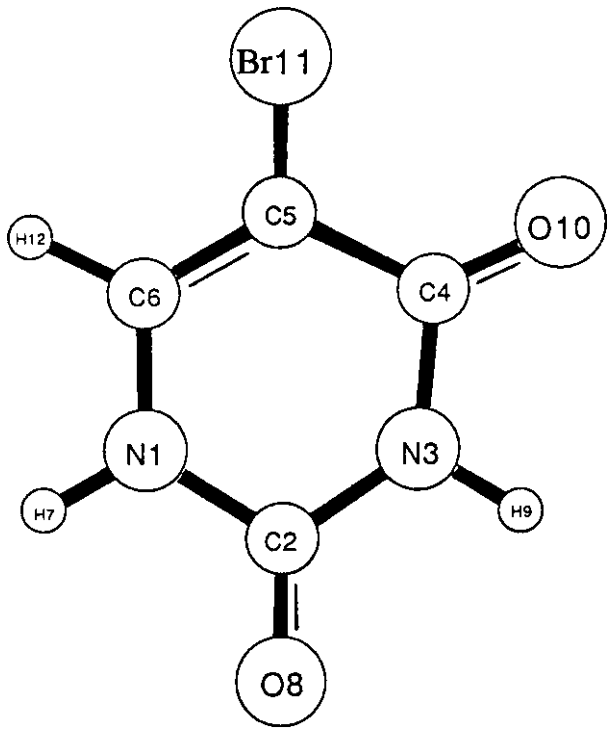

Figure 1. Labeling of the atoms in 5-BrU.

Except at the HF level, the calculated bond lengths appear very close to the ED results of uracil, while they differ remarkably with the X-ray data.[61–63] The calculated C═O bond lengths are sensitive to the inclusion of electron correlation. Its value is significantly underestimated by HF (1.19 *vs* 1.21 Å reported experimentally in the gas phase of uracil). As a result of H-bonding, the observed C═O bond length obtained by X-ray diffraction is about 0.02 Å longer than in the gas phase of uracil. The lengths of the C–N and C–C single bonds are intermediate between the corresponding aromatic and the saturated bonds, i.e. some aromatic character is on the ring structure.

With the increase of the basis set, the N–C, N–H, C═C and C═O bond lengths are slightly shortened, and the C–C–Br angle is slightly opened. Among the methods used, BLYP shows the longest calculated bond lengths. MP2 computes N–C, C═C, N–H, C═O and C–Br bond lengths remarkably longer than HF and much closer to B3LYP than to HF. The results with the aug-cc-pVTZ basis set are similar to those obtained by using 6-311++G(3df,pd) basis set.

The angles, in general, have not shown appreciable differences, at different levels, from those of the uracil molecule. The molecule is completely planar, so the torsional angles are 0 or 180°.

Hydrated form

Special attention has been paid to the hydration because the biological functions of nucleic acids are dependent on their interactions with the surrounding water. This interaction takes place through both hydrophilic and hydrophobic sites forming two hydration shells, clearly described in the bibliography. To simulate theoretically the hydration effects, three procedures have been suggested[64]: (1) empirical scaling of the quantum mechanical force constants of the isolated molecule;[65] (2) use of continuum model[66] or (3) modelling of the solvated compound by a molecular complex with water.[67] The continuum model procedure has a solid theoretical ground and is used mostly today, owing to mainly its simplicity and the lower computation time required. However, from a strictly theoretical point of view, the third procedure may be preferred, provided that the size of the considered complex is not too large. If this procedure is used with several water molecules, the first hydration shell can be better reproduced than by using the continuum model. Therefore, for high accuracy this procedure is preferred in the present work.

The presence of water is considered within a simple model with only one molecule, and in three positions, complexes A–C, which appear schematised at B3LYP level in Table 2, making two simultaneous H-bonds to an amino hydrogen and to a carbonyl oxygen. A small difference in energy appears among these conformations, the most stable one being the complex A. As in uracil molecule[42] and its derivatives[44] the relation of stability is:

complexes A > complexes C > complexes B.

DOI: 10.1002/jrs

Table 1. Geometrical parameters, bond lengths (in Å) and angles (in degrees) of 5-BrU

	HF					B3LYP							Uracil[a]		
Parameters	6–31G**	6–31++G**	MP2/ 6–31G**	BLYP/ 6–31G**	B3P86/ 6–31G**	6–31G**	6–311 + G (2d,p)	6–311++G (3df,pd)	aug-cc-pVDZ	aug-cc-pVTZ	B3PW91/ 6–31G**	MPW1 PW91/ 6–31G**	B3LYP/ aug-cc-pVTZ	X-ray[b]	Electron diffraction
Bond lengths															
N1–C2	1.3729	1.3719	1.3887	1.4099	1.3876	1.3935	1.3886	1.3875	1.3921	1.3877	1.3894	1.3861	1.3895	1.369(2)[c]	1.395(6)[c]
C2–N3	1.3702	1.3693	1.3869	1.4008	1.3811	1.3865	1.3819	1.3806	1.3856	1.3808	1.3824	1.3793	1.3794	1.369(2)[c]	1.391(6)[c]
N3–C4	1.3889	1.3887	1.4043	1.4273	1.4019	1.4087	1.4060	1.4051	1.4097	1.4050	1.4042	1.4006	1.4080	1.369(2)[c]	1.415(6)[c]
C4–C5	1.4704	1.4704	1.4661	1.4766	1.4641	1.4699	1.4648	1.4652	1.4700	1.4651	1.4660	1.4639	1.4546	1.430(3)	1.462(8)
C5═C6	1.3290	1.3301	1.3534	1.3640	1.3494	1.3513	1.3448	1.3448	1.3539	1.3450	1.3505	1.3478	1.3435	1.340(2)	1.343(24)
N1–C6	1.3694	1.3693	1.3751	1.3851	1.3692	1.3747	1.3718	1.3703	1.3761	1.3705	1.3702	1.3681	1.3709	1.3557[e]	1.396
N1–H	0.9944	0.9950	1.0084	1.0178	1.0088	1.0098	1.0087	1.0084	1.0112	1.0066	1.0089	1.0071	1.0062	–	1.002[d]
C2═O	1.1920	1.1941	1.2225	1.2281	1.2133	1.2157	1.2110	1.2092	1.2178	1.2107	1.2138	1.2111	1.2117	1.230(2)[c]	1.212(3)
C4═O	1.1889	1.1907	1.2237	1.2288	1.2132	1.2156	1.2102	1.2081	1.2163	1.2098	1.2136	1.2107	1.2143	1.230(2)[c]	1.211(3)
C–Br	1.8758	1.8670	1.8802	1.9073	1.8680	1.8847	1.8912	1.8856	1.8923	1.8866	1.8728	1.8684	–	1.86(2)[f]	–
Bond angles															
N–C2–N	113.52	113.58	112.30	112.17	112.69	112.63	112.90	112.84	112.96	112.84	112.62	112.71	113.06	114.0(1)	114.6(20)
C–N3–C	128.33	128.18	129.47	129.27	129.01	128.95	128.56	128.68	128.67	128.67	129.08	129.01	127.97	126.7(2)	126.0(14)
N–C4–C	113.08	113.43	112.27	112.17	112.59	112.60	112.90	112.80	112.78	112.81	112.52	112.60	113.61	115.5(1)	115.5(18)
C–C5═C	119.71	119.25	120.61	120.93	120.35	120.37	120.19	120.18	120.30	120.18	120.36	120.29	119.85	118.9(2)	119.7(21)
C2–N1–H	115.70	115.87	115.15	114.99	115.10	115.12	115.41	115.41	115.40	115.41	115.12	115.12	115.18	–	115.7[d]
N3–C2═O	123.62	123.56	124.28	124.78	124.33	124.38	124.15	124.18	124.12	124.19	124.38	124.31	124.22	122.3[e]	121.6[e]
C4–N3–H	116.02	116.09	115.39	115.38	115.62	115.59	115.77	115.69	115.72	115.70	115.55	115.59	116.32	–	–
N3–C4═O	120.89	120.62	121.25	120.80	120.98	120.87	120.58	120.64	120.57	120.63	120.95	120.98	120.23	119.1[e]	120.2
C4–C5–Br	118.46	118.85	117.95	117.89	117.82	117.97	118.28	118.30	118.31	118.30	117.92	117.91	118.23	–	118.1[d]
C5═C6–H	122.25	122.15	122.49	122.63	122.24	121.66	122.37	122.36	122.47	122.37	122.31	122.26	122.65	–	122.8[d]

[a] From Ref. 41.
[b] From Ref. 42.
[c] Mean value.
[d] Fixed parameter.
[e] Determined with the data reported in Refs 41,42.
[f] In bromobenzene [52,53].

Table 2. Equilibrium geometries at the B3LYP/6–311 + G(2d,p) level of hydrated 5-BrU with one water molecule. Bond lengths are in Å, and bond angles in degrees

Bond lengths	Complex A	Complex B	Complex C	Bond angles	Complex A	Complex B	Complex C	Interatomic angles	Complex A	Interatomic angles	Complex B	Interatomic angles	Complex C
N1–C2	1.3789	1.3831	1.3922	N–C2–N	113.90	114.00	113.19	N1–H···O13	144.98	N3–H···O13	143.85	N3–H···O13	144.99
C2–N3	1.3761	1.3728	1.3811	C2–N3–C4	128.17	127.76	127.77	C2═O···H15	108.75	C2═O···H15	109.17	C4═O···H15	111.27
N3–C4	1.4090	1.4058	1.3958	N3–C4–C5	112.67	113.14	113.92	H7···O–H14	135.06	H9···O–H14	131.45	H9···O–H14	131.93
C4–C5	1.4619	1.4673	1.4604	C4–C═C	120.18	120.28	119.91	H7···O–H15	85.14	H9···O–H15	85.77	H9···O–H15	84.64
C═C	1.3465	1.3436	1.3459	C2–N1–C6	123.05	123.43	123.75	O8···H15–O	142.64	O8···H15–O	141.37	O10···H15–O	142.34
N1–C6	1.3690	1.3735	1.3683	N3–C2═O	122.99	124.28	124.37	C2–N1–H7···O	−6.17	C2–N3–H···O	−5.45	C4–N3–H···O	−5.55
C2═O	1.2230	1.2224	1.2103	C4–N3–H	115.83	117.16	115.45	N1–H···O–H14	116.89	N3–H···O–H14	117.70	N3–H···O–H14	116.32
C4═O	1.2102	1.2094	1.2210	N3–C4═O	120.40	120.79	120.92	N1–H···O–H15	7.76	N3–H···O–H15	8.79	N3–H···O–H15	8.31
C5–Br	1.8919	1.8914	1.8919	C4–C5–Br	118.25	118.30	118.61	N1–C2═O···H15	1.88	N3–C2═O···H15	1.63	N3–C4═O···H15	1.54
RC[a] : A	1915	2128	1365	μ (Debye)	4.018	4.783	3.455	C2═O···H15–O	1.91	C2═O···H15–O	5.10	C4═O···H15–O	4.28
B	446	446	557[b]	Total En[b]	.962310	.959050	.959799	O8···H15–O–H14	−139.86	O8···H15–O–H14	−138.96	O10···H15–O–H14	−138.29
C	362	369	396	ZPE[c]	63.710	63.522	63.563	H7···O–H15···O8	−4.08	O8···H15–O···H9	−6.79	H9···O–H15···O10	−5.99

[a] Calculated rotational constants in MHz.

[b] −3064. (AU).

[c] Zero-point vibrational energy in Kcal/mol.

This fact has been attributed to the larger acidity of the N1–H bond than that of the N3–H bond and the larger basicity of the O8 atom than that of the O10 atom.[44] From the values of the total atomic charges (Table 6) it can be noted that the negative charge on O8 is slightly higher than that on O10, while on N1 it is lower than on N3. The positive charge on H9 is very close to that of H7 or slightly larger. These features lead to remarkably shorter O8···H15 and H7···O13 intermolecular bonds in complex A (i.e. the most stable) than those in complex C, which in turn are shorter than those in complex B.

The water molecule slightly changes the geometry and charge distribution. The main effect observed on hydration is lengthening of the N–H and C═O bonds involved in the intermolecular H-bonds by 0.01 Å. By contrast, the neighbours N–C bonds (or N–C and C–C, complex C) shrank by 0.005 Å. This resembles in behaviour of a typical amide bond in water (enhanced amide resonance due to solute–solvent interaction[68]). As expected, the C–H bonds are not sensitive to the presence of water, and the C–Br bond has a very small lengthening, 0.0007 Å. Under hydration, the carbonyl oxygen and the amino nitrogen involved in the H-bonds show more negative charge, by 0.04 and 0.06 respectively, while the hydrogen amino is more positive, by 0.08.

The data presented in Table 2 indicate that the intermolecular distances depend on the nature of the substituents implanted on the uracil ring. In uracil[42] the $OH_{water}\cdots O$ distances vary within the limits of 1.92–1.96 Å and the $NH\cdots O_{water}$ distance between 1.94 and 2.00 Å, while in 5-FU[44] the values are 1.96–1.99 Å and 1.92–1.97 Å, respectively. This fact has been discussed in terms of the proton affinities and deprotonation enthalpies of the bonds or atoms involved in the interaction with water.

The O13···H7 intermolecular bond in the complex A, 1.9165 Å, is slightly shorter than that corresponding to hydrated uracil,[42] 1.9400 Å, while the O8···H15 (1.9623 Å) is larger than in uracil, 1.9424 Å. Thus the H7···O–H15 angle is opened (85.14 *vs* 83.69° in uracil) and the O8···H15–O13 is closed (142.64 *vs* 144.47° in uracil). The H_2O molecule in complexes B and C is slightly rotated with a C4═O···H15–O angle of approximately 5°, while in complex A by approximately 2°. The values are analogous to uracil.[42]

Other hydration forms can also be formed with a water dimer instead of the water monomer, or complexes with different amounts of water, to reproduce the first hydration shell.[42] Another possibility could be through the bromine atom, with two simultaneous H-bonds to Br atom and to carbonyl oxygen. This possibility, pointed out by Del Bene[43] with low *ab initio* calculations for 5-FU, was not real in 5-BrU. Calculations performed at B3LYP/6-311+g(2d,p) level give rises to the form shown in Fig. 2, with the H_2O molecule placed symmetrically on the bromine atom, and with an intermolecular distance of 3.10 Å, far for the consideration of an intermolecular H-bond.

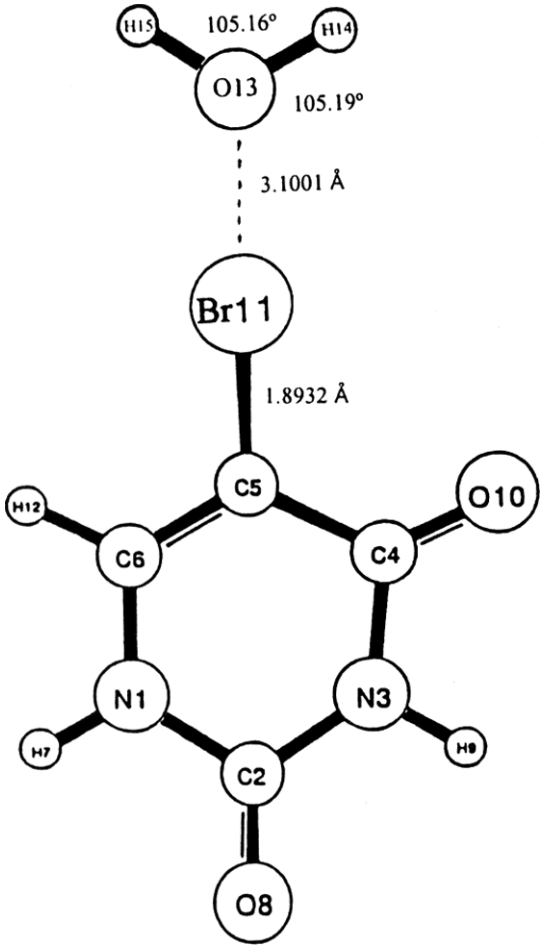

Figure 2. Optimum form computed by B3LYP/6-311++G(2d,p) for the interaction of bromine atom with one H_2O molecule.

Rotational constants, dipole moments, energy and harmonic ZPE for each system are also included at the bottom of Table 2. As in the uracil molecule,[42] a significantly higher dipole moment is predicted for the complex B (the less stable) than for the complex A (the most stable). Complex C has the lowest dipole moment but it is only slightly more stable than complex B.

Vibrational wavenumbers

The present molecule belongs to the C_s point group with the normal mode distribution $21a' + 9a''$. According to the selection rules, both a' and a'' vibrations are allowed in Raman and IR spectra; a' vibrations are totally symmetric and give rise to polarized Raman lines, whereas a'' vibrations are antisymmetric and give rise to depolarized Raman lines.

The vibrational bands computed with our theoretical methods are shown in Table 3. The first and second columns list their calculated wavenumbers at the HF/6-31G** and HF/6-31++G** levels with their relative infrared intensities (the third column), their Raman activities (the fourth column) and the depolarization ratios (the fifth column). The relative

DOI: 10.1002/jrs

intensities (and activities) were obtained by normalising the computed value to the intensity of the strongest line. The 6–19th columns collect the calculated values with the MPW1PW91, B3P86, B3LYP and B3PW91 methods. In the last column appears the percentage contribution of the different modes to a computed wavenumber. Contributions lower than 10% were not considered. The correspondence with the uracil ring modes[36] appears in the previous column. It is observed that most of the vibrational wavenumbers arise on account of mixing of different normal modes.

The observed IR and FT-Raman lines of 5-BrU along with their relative intensities are collected in Table 4. The IR data have been reported in Ar-matrix by Graindourze *et al*.,[33,34] Szczesniak *et al*.[69] and Nowak *et al*.,[70] columns 15–16th, and Raman lines by Rai,[32] column 19. Our results in the solid state, columns 17–18, complete these data specially in the low-wavenumber region. For simplicity, the last column with the assignments include only the contributions of the predominant modes. Figures 3 and 4 show respectively, the FTIR and FT-Raman spectra of 5-BrU recorded in the solid state.

For comparison with our theoretical calculations, with experimental only those wavenumbers were selected that were reported in Ar-matrix,[69,70] but complemented with the values of Graindourze *et al*.[33,34] and our Raman data. One may note that the computed wavenumbers correspond to Ar-matrix or to solid state. Remarkable differences appear among these data. The intermolecular forces present in the solid state play a dominant role in modifying the magnitudes and intensities of the wavenumbers. However, in Ar-matrix these forces are very low and therefore their wavenumbers were selected for the comparison, and thus a satisfactory one-to-one correspondence can be established in Table 4. The intensity of a band is another factor for its selection. Thus the experimental band[37] at 3058 cm^{-1} was chosen instead of the weak band[33,34] at 3040 cm^{-1}. This selection was in accordance with our theoretical calculations. Table 4 also shows the revised assignment of several infrared bands, e.g. the band at 906 cm^{-1} was reassigned as γ(C6–H) instead of ring.[33,34]

The assignments for several modes are obvious and require no further discussion and therefore only a brief analysis is given here. A general analysis of the different modes is as follows:

N–H modes

Three fundamental modes are expected to appear above 3000 cm^{-1}, namely (C–H), (N1–H) and (N3–H) stretching modes. The C–H stretching appears in the 3030–3080 cm^{-1} range, while the N–H stretches are in 3420–3490 cm^{-1} range. These modes are essentially pure group modes, and are comparable to uracil or its other derivatives[42,71]; the substitution only induces shifts of about 1% or less. The N–H stretching modes were calculated with medium IR intensity in accordance with the experimental results. Also, these modes were determined as the strongest Raman bands in contrast to their non-detection in the Raman spectrum, and may be due to fluorescence. In 5-FU the strongest Raman intensity corresponds to the C6–H stretching. The predicted values for the (N–H) stretching modes agree well with the Ar-matrix data.[33,34] Considerable lowering of the wavenumber of these modes is observed in the solid state, indicating the presence of strong intermolecular forces in 5-BrU. The lower magnitude of the stretching (N3–H) vibrational mode is due to the involvement of the H-atom at the N3 position in the hydrogen bonding (with the O atom at the C4 position) of the type C=O···H-N.

The N-H in-plane bendings are highly coupled to the other group or ring modes.

C=O modes

The typical pattern of the absorption bands due to the C=O stretching vibrations of uracil and its derivatives is always very complex, and appears as very broad and strong IR bands. The C2=O vibrational mode was calculated by the DFT methods with the strongest IR intensity, which agrees with the experimental value and higher than that of C4=O vibrational mode. By contrast, by using HF the mode, C4=O appears at a higher intensity than C2=O. In the uracil molecule,[71] mode C4=O appears by HF and DFT methods with higher IR intensity than that of C2=O mode, although by DFT methods the difference in IR intensity is very small while by HF it is very high (approximately 3 times). A small coupling is determined among the C2=O, C4=O and N–H modes. Under substitution, the mode remains almost unchanged, and thus the calculated wavenumbers of the C=O modes in 5-BrU is observed close to uracil, only few cm^{-1} higher, and they shift towards lower wavenumbers under hydration.

The oxygen atom at the C4 position is involved in hydrogen bonding and therefore, the C2=O stretching mode is expected to appear at a higher wavenumber than the C4=O mode. The lower wavenumber of this mode in the solid state and its broad intensity are due to different and strong intermolecular forces through this group.

The planar bending modes due to C2=O and C4=O bonds are assigned at lower wavenumbers than the corresponding non-planar bending modes.

C–Br modes

The predicted C–Br stretching vibration at approximately 620 cm^{-1} is in range reported in the literature,[72] 545 ± 75 cm^{-1}. The in-plane C–Br deformation predicted at approximately 290 cm^{-1} is also in accordance with the literature values, 300 ± 60 cm^{-1}, and it was assigned to the band detected at 300 cm^{-1}. However, the out-of-plane (C–Br) deformation is predicted at approximately 100 cm^{-1}, far from the 230 ± 65 cm^{-1} range reported for this mode as such the Raman band at 101 cm^{-1} has been assigned to this mode.[72]

C=C and ring modes

The wavenumber of the (C=C) stretch is slightly lowered with the 5-X substitution of uracil, with the exception of 5-FU.

DOI: 10.1002/jrs

Table 3. Vibrational wavenumbers (in cm^{-1}) obtained in 5-BrU at different theoretical levels

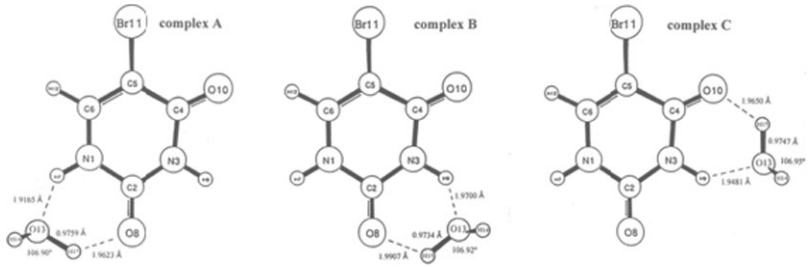

HF[b]					MPW1PW91		B3P86	B3LYP[f]									B3PW91			Uracil	
wav.[a]	wav.	I[c]	A[d]	Dep.[e]	wav.[a]	I[c]	wav.[a]	wav.[j]	wav.[a]	wav.	I[c]	A[d]	Dep.[a,e]	Dep.[e]	Red.[g]	forc.[h]	wav.[a]	I[c]	sym.	mode	Characterisation[i]
3896	3888	13	100	.19	3702	19	3679	3628.3	3653	3632.7	17	100	.23	.19	1.08	8.39	3677	18	a′	30	100%, ν(N1–H)
3858	3847	9	69	.23	3663	13	3639	3585.0	3616	3589.5	11	76	.28	.23	1.08	8.18	3638	12	a′	29	100%, ν(N3–H)
3410	3405	0	67	.33	3267	0	3248	3225.4	3237	3213.7	0	62	.34	.31	1.09	6.66	3247	0	a′	27	100%, ν(C6–H)
2017	1987	53	35	.12	1885	100	1870	1794.7	1847	1793.3	100	14	.21	.18	7.99	15.14	1867	100	a′	26	78%, ν(C2═O) + 11%, ν(C4═O) + 10%, δ(N–H)
2001	1971	100	24	.56	1848	67	1831	1761.6	1808	1759.1	65	24	.33	.38	9.20	16.77	1828	65	a′	25	76%, ν(C4═O) + 11%, ν(C2═O) + 10%,δ(N3–H)
1846	1839	15	66	.14	1708	11	1695	1665.5	1679	1662.0	11	36	.17	.14	5.51	8.96	1692	11	a′	24	70%, ν(C5═C6) + 20%, ν(ring)
1641	1638	10	12	.59	1519	16	1507	1484.4	1493	1486.1	12	10	.59	.49	2.44	3.18	1505	15	a′	23	60%, δ(N1–H) + 38%, ν(ring)
1547	1547	6	4	.36	1437	14	1425	1404.0	1411	1408.8	13	2	.54	.61	2.11	2.47	1423	14	a′	22	65%, ν(ring) + 30%, δ(N1–H)
1560	1559	11	1	.69	1412	2	1400	1392.4	1396	1399.8	5	1	.71	.75	2.50	2.89	1400	2	a′	21	75%, δ(N3–H) + 14%, δ(N1–H) + 10%, δ(ring)
1482	1482	1	42	.28	1369	1	1359	1342.7	1353	1346.6	2	22	.33	.26	1.83	1.96	1357	1	a′	20	65%, δ(C6–H) + 20%, ν(ring) + 13%, δ(N1–H)
1328	1330	6	2	.47	1223	6	1211	1193.8	1196	1191.6	12	1	.52	.58	1.89	1.58	1208	8	a′	19	60%, δ(N1–H, C6–H) + 38%, ν(ring)
1255	1255	9	1	.14	1195	9	1187	1162.7	1170	1156.1	3	2	.74	.66	4.37	3.44	1185	7	a′	18	52%, ν(N1–C6) + 46%, ν(ring)
1147	1154	6	3	.25	1073	8	1063	1049.7	1053	1055.2	8	1	.28	.29	7.07	4.64	1062	8	a′	17	100%, ν(ring)
1062	1063	1	5	.56	989	1	981	970.4	971	970.8	2	2	.66	.64	3.00	1.66	979	2	a′	14	32%,δ(N3–H) + 28%,δ(C6–H) + 15%,ν(C–N)+18%, δ(ring)

1074	1124	1	2	.75	937	2	927	921.8	928	926.0	2	2	.75	.75	1.39	.70	926	2	a″	15	97%, γ(C6–H)
840	839	1	12	.05	790	0	784	772.1	777	778.5	0	19	.11	.74	9.23	3.30	783	0	a′	12	100%, v(ring)
872	900	3	2	.75	788	5	782	772.5	776	773.5	4	1	.75	.07	9.00	3.17	781	5	a″	10	60%, γ(C4═O) + 40%, γ(N3–H)
852	849	7	0	.75	763	8	755	755.5	748	757.8	8	0	.75	.75	10.62	3.59	754	8	a″	11	53%, γ(C2═O) + 34%, γ(C4═O) + 13%, γ(ring)
726	738	8	1	.75	689	11	685	691.0	681	667.5	12	3	.75	.75	1.15	0.30	684	11	a″	9	68%, γ(C–N3–H) + 32%, γ(ring)
680	683	4	2	.18	635	6	630	625.7	626	629.2	6	1	.56	.34	7.20	1.68	630	6	a′	–	75%, δ(ring) + 20%, v(C–Br)
650	648	0	6	.25	604	0	600	593.6	598	597.6	0	5	.37	.28	6.61	1.39	600	0	a′	7	60%, δ(ring) + 40%, δ(C═O)
591	595	6	0	.75	576	10	574	585.7	567	551.3	9	2	.75	.75	1.11	0.20	573	10	a″	8	98%, γ(N1–H)
587	588	1	4	.20	542	1	538	535.8	536	539.5	2	3	.32	.22	8.23	1.41	537	1	a′	6	100%, δ(ring)
437	436	3	2	.55	400	3	397	393.5	395	397.0	3	2	.57	.48	12.29	1.14	396	3	a′	3	53%, δ(C═O) + 35%, δ(ring)
429	488	3	1	.75	396	3	393	393.8	392	388.1	3	2	.75	.75	2.91	0.26	393	3	a″	4	68%, γ(C–H) + 32%, γ(ring)
306	309	0	5	.27	291	0	289	283.3	285	283.9	0	3	.32	.26	18.26	0.87	288	0	a′	–	70%, δ(C–Br) + 30%, δ(ring)
304	352	1	0	.75	286	0	284	274.4	281	268.2	0	0	.75	.75	11.29	0.48	284	0	a″	–	75%, γ(NCC) + 25%, γ(C–H)
201	198	0	1	.72	187	0	185	183.3	186	183.2	0	1	.73	.72	13.00	0.26	185	0	a′	–	80%, δ(C–Br) + 20%, δ(ring)
168	170	0	0	.75	155	0	155	154.2	153	148.7	0	0	.75	.75	8.75	0.11	154	0	a″	1	67%, γ(C═O) + 18%, γ(ring)
96	97	0	0	.75	92	0	91	89.8	91	87.2	0	1	.75	.75	10.84	0.05	92	0	a″	–	37%,γ(C═O) + 29%,γ(C–Br) + 22%,γ(N1–H) +12%,γ(ring)

[a] With the 6–31G** basis set.
[b] With the 6–31++G** basis set.
[c] I, relative infrared intensities in %.
[d] A, relative Raman intensities in %.
[e] Raman depolarization ratios.
[f] With the 6–311 + G(2d,p) basis set.
[g] Reduced mass (amu).
[h] Force constants (mdyneÅ^{-1}).
[i] By B3LYP/6–311 + G(2d,p).
[j] With the aug-cc-pVDZ basis set.

DOI: 10.1002/jrs

Table 4. Scaled wavenumbers (in cm^{-1}) by several procedures in 5-BrU with the 6–31G** basis set

With an overall scale factor[a]		With one scaling equation[b]					With two scaling equations[f]		With specific scale factors[b]					Experimental[g]					Uracil mode	Assignment
HF	B3LYP	HF	B3LYP	B3LYP[c]	B3LYP[d]	MPW1 PW91[e]	B3LYP[c]	MPW1 PW91	HF	B3P86	B3LYP	B3LYP[c]	MPW1 PW91	IR[h]	IR[i]	IR[j]	Raman[j]	Raman[k]		
3503	3513	3484	3486	3496	3491	3488	3478	3475	3479	3481	3479	3481	3481	3459	3471[m]	–	–	–	30	ν(N1–H)
3469	3476	3450	3451	3454	3450	3452	3438	3441	3432	3432	3432	3434	3433	3413	3425[m]	3346 w?	–	–	29	ν(N3–H)
3066	3111	3050	3093	3096	3107	3082	3093	3092	3090	3089	3091	3089	3090	3058[l,m]	–	3055vs 2904vs 2344s	3052.0 2895.6w	3058	27	ν(C6–H)
1814	1776	1806	1779	1741	1741	1792	1760	1796	1760	1758	1758	1758	1760	1761[m]	–	1682br	1675.3vs	1770	26	υ(C2=O)
1799	1738	1792	1743	1709	1710	1758	1727	1761	1746	1742	1741	1743	1743	1729[m]				1675	25	υ(C4=O)
1660	1614	1654	1621	1616	1618	1627	1632	1630	1640	1632	1630	1633	1633[m]	1635[m]	–	–	1618.1s 1495.0m	– 1496	24 –	υ(C5=C6) –
1476	1435	1471	1445	1448	1445	1451	1461	1453	1456	1449	1448	1449	1449	1463	1458[m]	1440s	1450.2w	1447	23	δ(N1–H) + υ(ring)
1391	1357	1387	1368	1375	1368	1374	1385	1376	1391	1397	1389	1386	1397	1400	1390[m]	–	1405.6m	1427	22	υ(ring) + δ(N1–H)
1403	1342	1398	1353	1366	1357	1351	1377	1353	1392	1370	1376	1381	1373	1397	1377[m]				21	δ(N3–H)
1333	1301	1329	1313	1315	1310	1311	1325	1312	1313	1328	1328	1321	1326	1327[m]	–	1342s	1340.7vs	1350	20	δ(C6–H) + υ(ring)[n]
1194	1150	1191	1164	1167	1168	1174	1174	1175	1170	1159	1153	1153	1162	1192	1189[m]	1229vs	1181.1w	1255	19	δ(N1–H, C6–H) + υ(ring)[n]
1128	1124	1126	1140	1133	1138	1148	1139	1149	1126	1150	1145	1138	1149	–	1154[m]				18	υ(N1–C6) + υ(ring)
1031	1007	1030	1029	1037	1030	1034	1041	1035	1047	1039	1036	1043	1041	1055	1048[m]	1060s	1053w	1060	17	υ(ring)
955	934	954	952	957	955	956	958	956	960	958	958	961	960	962?[m]	–	1004m	1014w	1008	14	δ(N3–H, C6–H)+υ(C–N)[n]
966	892	965	911	914	908	907	915	907	941	928	930	926	927	906?[m]	–	943m 870br	945.4w –	– 872	15 –	γ(C6–H) –
763	777	756	769	773	765	770	771	770	792	785	787	792	786	–	–	–	747.5w	–	12	υ(ring)
793	777	784	768	769	766	768	766	768	779	766	763	762	766	760[m]	–	778s	–	873	10	γ(C4=O) + γ(N3–H)[n]
774	749	766	741	754	750	745	751	744	748	752	753	750	752	753?[m]	–	755s	785.1vs	750	11	γ(C2=O) + γ(C4=O)[n]
660	681	654	678	667	688	676	663	675	656	652	654	651	653	656[m]	–	646vs	633.9	–	9	γ(C–N3–H) + γ(ring)[n]
618	624	613	626	631	626	625	625	624						626[m]	–	615w	609.8s	–	–	δ(ring) + υ(C–Br)[n]
591	599	586	600	601	595	596	595	595	597	599	599	597	599	594[m]	–	–	547.9s	580	7	δ(ring) + δ(C=O)

537	567	533	570	557	588	570	549	569	548	548	549	549	547	548[m]	–	546vs	–	560	8	γ(N1–H)
534	537	530	541	545	540	539	538	537	531	531	531	533	532	532[m]				545	6	δ(ring)
																442s				
397	396	396	408	409	404	406	399	404	401	403	401	401	403	390[m]	–	419w	423.8m	425	3	δ(C=O) + δ(ring)[n]
390	392	389	405	401	404	402	390	400	395	391	391	388	391					390	4	γ(C–H) + γ(ring)[n]
278	283	279	304	302	299	304	289	302								–	300.4m	–	–	δ(C–Br) + δ(ring)0[n]
276	279	277	300	287	290	300	273	297												γ(C=H) + γ(ring)[n]
183	184	185	210	206	204	207	191	204									201.0m	–	–	δ(ring) + δ(C=Br)
																	138.5vs			
153	153	156	179	173	176	177	157	174									125.6vs	–	1	γ(C=O) + γ(ring)[n]
87	90	91	121	114	114	119	97	115									101.1vs	–	–	γ(C=O,C–Br)+γ(N1–H)[n]
																	79.7m			
																–				

[a] With 0.8992 (HF) and 0.9614 (B3LYP), and for low-wavenumber vibrations (<800 cm^{-1}), 0.9089 (HF) and 1.0013 (B3LYP), Ref. 49,50.

[b] From Refs 27,48.

[c] With the 6–311 + G(2d,p) basis set.

[d] With the aug-cc-pVDZ basis set; the scaling equation used was: $\nu^{scal.} = 28.6 + 0.9543\ \nu^{cal.}$.

[e] With the equation: $\nu^{scal.} = 32.7 + 0.9334\ \nu^{cal.}$.

[f] With the scaling equations: $\nu^{scal.} = 12.0 + 0.9749\ \nu^{cal.}$ ($\nu^{cal.} < 2000\ cm^{-1}$) and $\nu^{scal.} = 141.4 + 0.9184\ \nu^{cal.}$ ($\nu^{cal.} > 2000\ cm^{-1}$) for B3LYP/6–311 + G(2d,p); and with $\nu^{scal.} = 28.9 + 0.9375\ \nu^{cal.}$ ($\nu^{cal.} < 2000\ cm^{-1}$) and $\nu^{scal.} = 218.8 + 0.8796\ \nu^{cal.}$ ($\nu^{cal.} > 2000\ cm^{-1}$) for MPW1PW91.

[g] Note: *vs*, very strong; s, strong; m, medium; w, weak; br, broad.

[h] In Ar-matrix, Ref. 22.

[i] Ref. 51.

[j] Present work.

[k] Ref. 21.

[l] From Ref. 25.

[m] Value selected for the theoretical comparison.

[n] Low contribution of this mode.

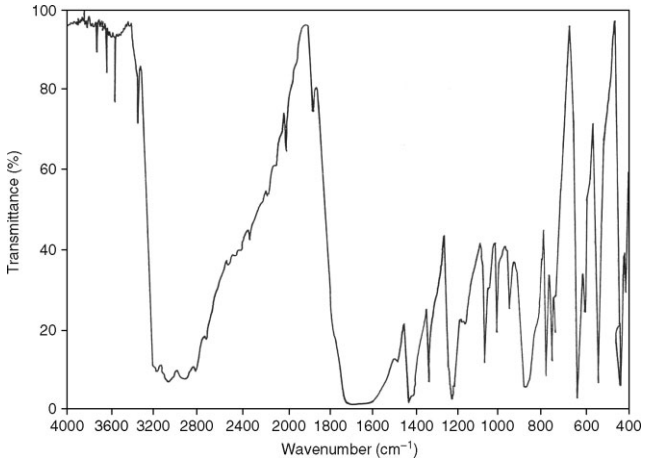

Figure 3. Infrared spectrum of 5-BrU in solid state.

The null IR intensity predicted for mode 12 is in accordance with the lack of bands in the IR spectra, but it was computed with medium Raman intensity and therefore it was observed at 747.5 cm^{-1}.

Several combination and overtone lines were also observed, and are included in Table 4.

Scaling

Table 5 shows the rms (root-mean-square) errors obtained with the different methods and basis sets used in the present work. The second column shows the error in the calculated wavenumbers. It is noted that a remarkably large error is obtained by HF, while BLYP gives the lowest errors. The HF calculated results are usually more overestimated than the corresponding DFT ones, but even with these DFT methods the error is too large for an accurate comparison of our calculated wavenumbers with the experimental ones. Therefore, scaling is required.

It is well known that the calculated HF and DFT harmonic wavenumbers could significantly overestimate experimental values because of a lack of electron correlation, insufficient basis sets or anharmonicity. Much effort has been made to reproduce accurately the experimental wavenumbers in theoretical calculations. Both uniform and individual scaling of force constants and/or wavenumbers have been the subject of substantial discussion in the literature.[42,71,73] These scaling procedures are based on the transferability of the force constants and/or the wavenumbers among similar molecules and characteristic groups.

Table 5. Errors (rms)* obtained in the calculated and scaled wavenumbers of 5-BrU by the different procedures, methods and levels

Method	(a)	(b)	(c)	(d)	(e)
HF/6–31G**	181	26.6	23.5	21.9	17.0
HF/6–31++G**	179	–	28.6	27.9	26.9
BLYP/6–31G**	40	38.5	27.0	19.6	19.5
B3P86/6–31G**	76	25.4	19.5	18.3	14.2
B3LYP/6–31G**	67	25.9	18.7	16.6	15.2
B3LYP/6–311 + G(2d,p)	55	–	18.6	15.0	15.6
B3LYP/aug-cc-pVDZ	–	–	–	14.4	14.2
B3PW91/6–31G**	75	26.2	19.6	18.4	14.2
MPW1PW91/6–31G**	86	–	19.0	18.3	13.9

rms*, defined as $(\Sigma(\omega^{cal} - v^{exp})^2/n)^{1/2}$, where the sum is over all the modes, n, and v^{exp} is from the second column: (a) calculated wavenumbers; (b) scaled wavenumbers with an overall factor; (c) scaled with one scaling equation; (d) scaled with two scaling equations; (e) scaled wavenumbers with specific scale factors for each mode.

To improve the computed wavenumbers, in Table 4 appears the scaled wavenumbers obtained by four procedures.[71] With the first one, all the computed wavenumbers at a specific level of theory were multiplied by a uniform scale factor.[74] Another scale factor is required to be used for wavenumbers lower than 800 cm^{-1}. Scale factors have been reported only for a few basis sets,[74] and therefore this procedure was not applied to several levels used in the present work. The results obtained by HF and B3LYP methods by applying this scaling are shown in the 1st and 2nd columns of Table 4. With this procedure error is remarkably reduced, and the values obtained with the different methods used are shown in the 3rd column of Table 5. With HF, the reduction is so large that the scaled wavenumbers are of

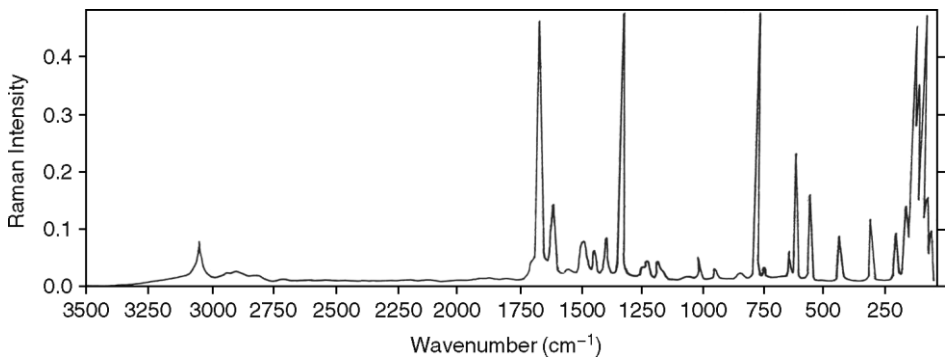

Figure 4. Raman spectrum of 5-BrU in solid state.

DOI: 10.1002/jrs

accuracy comparable to B3-methods. In B-based procedures a significant improvement with the scaling is not observed and they have the largest errors. However, with B3-based procedures, the errors are remarkably reduced and they are close to HF; but in both cases the errors are larger than the required accuracy. A noticeable improvement is obtained with the use of a scaling equation.

The second scaling procedure uses specific scaling equations obtained previously from the uracil molecule.[71] The results obtained with HF, B3LYP, B3PW91 and MPW1PW91 methods are listed in the 3rd to 7th columns of Table 4, while the rms errors are shown in the 4th column of Table 5. An improvement of approximately 20% is achieved over the overall scale factor procedure.

With the use of the scaling equation approach, the low-wavenumber vibrations are usually predicted fairly accurately, while stretching wavenumbers appear overestimated. By dividing the wavenumber range into two parts, and using one scaling equation for the 0–2000 cm^{-1} range and another one for the 2000–4000 cm^{-1} range, the error in the stretching region is remarkably reduced.[68] These equations were obtained by linear fittings of the values for the uracil molecule. Thus the main purpose of this third procedure is to improve the scaled stretching wavenumbers. The scaled values for B3LYP and MPW1PW91 are shown in the 8th–9th columns of Table 4, while the rms errors obtained appear in the 5th column of Table 5. A significant improvement is reached in 5-BrU, and notoriously in the uracil molecule with a reduction of 33% error over one scaling equation (rms of 9.1 *vs* 13.7).

Again a new improvement can be carried out on the computed wavenumbers if specific scale factor procedures are used. The scaled values obtained using this fourth scaling procedure are listed in the 10th–14th columns of Table 4 and the rms errors in the last column of Table 5. This scaling leads to the lowest errors. Individual scaling is however more complex and time consuming, and thus this approach is less recommended to be used, except for special cases.

An overall conclusion is that the increase of the basis set has a small effect and the calculations with B3-based methods and with the 6-31G** basis set appear in general to be useful with the best cost effective relationships, when they are combined with an adequate scaling procedure.

OTHER MOLECULAR PROPERTIES

The values of the Mulliken charge obtained with the theoretical methods used are listed in Table 6. Close values are obtained between HF and MP2 *ab initio* methods, but they differ considerably with the DFT results. Appreciable differences in values are also noted among the BLYP, B3P86 and B3LYP methods.

Several thermodynamic parameters were also calculated and collected in Tables 7 and 8. For an accurate prediction in determining the ZPVE (zero-point vibrational energies), the enthaply $H_{vib}.(T)$, and the entropy $S_{vib}.(T)$, scale factors has been reported[74] for the 6-31G* basis set. Dipole moments have been reported[75] only for different excited states of 5-BrU.

A replacement of the H11 atom by fluorine in 5-FU[3] produces a slightly higher change of the local charge distribution than the replacement by bromine atom. However, the calculated dipole moment by HF and MP2 in 5-FU[3] is lower than in 5-BrU, while by B3P86 and B3LYP it is slightly higher. Compared to uracil, the dipole moment in 5-BrU is very much lower, e.g. at the B3LYP/6-311+G(2d,p) level is 4.518 D in uracil and 4.028 D in 5-BrU. It is noted that with the 6-31G** basis set, the value is overestimated by MP2 (4.57 D) and slightly underestimated by DFT methods. The increase of the basis set remarkably improves the calculated values, which are more in accordance with the experimental ones,[76]

Table 6. Total atomic charges on the atoms

	HF				B3LYP					
Atoms	6–31G**	6–31++G**	MP2/ 6–31G**	B3P86/ 6–31G**	6–31G**	6–311 + G (2d,p)	6–311++G (3df,pd)	aug-cc-pVTZ	B3PW91/ 6–31G**	MPW1PW91/ 6–31G**
N1	−0.785	−0.628	−0.786	−0.613	−0.568	−0.409	−0.981	0.015	−0.615	−0.628
C2	1.025	0.913	1.038	0.781	0.750	0.659	1.391	0.147	0.787	0.804
N3	−0.836	−0.738	−0.843	−0.654	−0.606	−0.492	−0.964	0.186	−0.658	−0.672
C4	0.853	0.281	0.862	0.639	0.611	0.268	1.045	0.391	0.646	0.662
C5	−0.245	0.264	−0.242	−0.105	−0.061	0.482	0.004	0.146	−0.118	−0.134
C6	0.257	−0.104	0.260	0.144	0.152	−0.329	0.369	−0.373	0.149	0.157
H7	0.349	0.401	0.355	0.321	0.296	0.282	0.304	0.044	0.320	0.322
O8	−0.589	−0.598	−0.605	−0.495	−0.487	−0.482	−0.783	−0.634	−0.495	−0.501
H9	0.354	0.418	0.360	0.323	0.298	0.285	0.314	0.080	0.322	0.325
O10	−0.554	−0.518	−0.578	−0.476	−0.471	−0.444	−0.766	−0.633	−0.475	−0.480
Br11	−0.046	0.101	−0.043	−0.052	−0.068	0.036	−0.088	0.072	−0.049	−0.046
H12	0.217	0.208	0.224	0.187	0.155	0.144	0.155	0.561	0.187	0.192

DOI: 10.1002/jrs

Table 7. Theoretical computed total energies (A.U.), zero-point vibrational energies (Kcal mol^{-1}) and dipole moments (Debyes) in 5-BrU

Methods	Total energy (RH)	Zero-point energy	Dipole moments
HF/6–31G**	−2981.77893	52.698	4.278
HF/6–31++G**	−2981.81314	52.862	4.436
MP2/6–31G**	−2981.77257	–	4.574
B3P86/6–31G**	−2987.75006	48.836	3.907
B3LYP/6–31G**	−2985.92184	48.468	3.868
B3LYP/6–311 + G(2d,p)	−2988.48631	48.095	4.028
B3LYP/6–311++ G(3df,pd)	−2988.51390	–	3.987
B3LYP/aug-cc-pVDZ	−2988.43186	48.158	4.035
B3LYP/aug-cc-pVTZ	−2988.60290	–	3.978
B3PW91/6–31G**	−2985.75074	48.789	3.896
MPW1PW91/6–31G**	−2985.98067	49.204	3.917

4.1 ± 0.01 D. The addition of diffuse functions increases the value of the dipole moment.

SUMMARY AND CONCLUSIONS

The calculated structure for 5-BrU appears coherent in comparison with the experimental values reported for uracil, with all the values well within the uncertainties of the methods used. The geometries and values of the properties presented here appear to be the most accurate to date.

The structural and characteristics of the first hydration shell were analyzed through realistic molecular models. The three stable complexes determined with one water molecule are the ones in which the oxygen atom of water accepts the acidic NH proton while donating a proton to the carbonyl oxygen. The presence of water molecule increases harmonic vibration intensities of 5-BrU, and both C═O and N–H stretching wavenumbers appear at lower values.

The accuracy of different *ab initio* methods in predicting the spectra was compared. To improve the calculated wavenumbers, three procedures were used. The scaling equation procedure gives rise to a slight improvement in the predicted wavenumbers, when a single overall scale factor is used. With the use of two scaling equations a significantly better accuracy is obtained for the predicted stretching wavenumbers. Use of scale factors transferred from uracil molecule permits us to make an *a priori* prediction of the IR and Raman bands of 5-BrU of sufficient quality to confirm many of the previously assigned fundamental modes and to suggest several alterations. After proper scaling the computed wavenumbers were in good agreement with the observed wavenumbers, except in a few cases. However, the computed intensities show marked deviations form the observed values.

B3-based DFT procedures with 6-31G** basis set provide a very cost-effective means of determining harmonic wavenumbers. They show better results than HF-and MP2-based procedures.

The bromine atom at position 5 exhibit smaller inductive effect than the fluorine atom, producing a small distortion of the electrostatic potential around the ring and a reduction of the molecular dipole moment.

REFERENCES

1. Morris SM. *Mutat. Res.* 1993; **297**: 39.
2. Dobrosz-Teperek K, Zwierzchowska Z, Lewandowski W, Bajdor K, Dobrowolski JCZ, Mazurek AP. *J. Mol. Struct.* 1998; **471**: 115.
3. Rastogi VK, Jain V, Yadav RA, Singh C, Alcolea Palafox M. *J. Raman Spectrosc.* 2000; **31**: 595.
4. Schmittgen TD, Danenberg KD, Horikoshi T, Lenz HJ, Danenberg PV. *J. Biol. Chem.* 1994; **269**: 16269.
5. Rastogi VK, Singh C, Jain V, Alcolea Palafox M. *J. Raman Spectrosc.* 2000; **31**: 1005.
6. Henderson JP, Byun J, Takeshita J, Heinecke JW. *J. Biol. Chem.* 2003; **278**: 32834.
7. Jiang Q, Bloun BC, Ames BN. *J. Biol. Chem.* 2003; **278**: 32834.
8. Denfil S, Ptasinsxa S, Gstir B, Scheier P, Mark TD. *Int. J. Mass Spectrom.* 2004; **232**: 99.

Table 8. Calculated values of rotational constants (GHz) and entropies (cal mol^{-1} K^{-1})

Parameters	HF/ 6–31++G**	MP2/ 6–31G**	B3LYP/ 6–311++G(3df,pd)	B3LYP/ aug-cc-pVTZ	B3PW91/ 6–31G**	MPW1PW91/ 6–31G**
Rotational constants	3.036	2.963	2.986	2.985	2.979	2.993
–	0.655	0.645	0.646	0.645	0.648	0.651
–	0.538	0.529	0.531	0.530	0.532	0.535
Entropy: Total	86.53	–	89.07[a]	88.85[b]	88.64	88.46
Translational	41.63	–	41.63[a]	41.63[b]	41.63	41.63
Rotational	30.09	–	30.14[a]	30.16[b]	30.13	30.11
Vibrational	14.81	–	17.30[a]	17.06[b]	16.89	16.71

[a] With the 6–31 + G(2d,p) basis set.
[b] With the aug-cc-pVDZ basis.

DOI: 10.1002/jrs

9. Ogino H, Fujii M, Satou W, Suzuki T, Michishita E, Ayusawa D. *DNA Res.* 2002; **9**: 25.
10. Katouzian-Safadi M, Charlier M. *Biochimie* 1994; **76**: 129.
11. Seki K, Ohkura K. *Radioisotopes* 1996; **45**: 227.
12. Katouzian-Safadi M, laine B, Charlier F, Cremet JY, Belaiche D, Sautiere P, Charlier M. *Nucleic Acids Res.* 1991; **19**: 4937.
13. Chattapadhyay MK, Sengupta D, Sengupta S. *Med. Sci. Res.* 1995; **775**: 775.
14. Grahn E, Moss T, Helgstrand C, Fridborg K, Sundaram M, Tars K, Lago H, Stonehouse NJ, Davis DR, Stockely PG, Liljas L. *RNA Pubi, RNA Soc.* 2001; **7**: 1616.
15. Henderson JP, Byun J, William MV, Mueller DM, Mc Cormick ML, Heinecke JW. *J. Biol. Chem.* 2001; **276**: 7867.
16. Hanawalt PC. *Mutat. Res. DNA Repair* 2001; **485**: 1.
17. Ferrer E, Shevchenko A, Eritja R. *Bioorg. Med. Chem.* 2000; **8**: 291.
18. Singh UP, Ghose R, Ghose AK, Si RK, Geeta B, Sodhi A. *Indian J. Cancer Chemother.* 1991; 33.
19. Rastogi VK, Singh A, Chawla SC, Gupta SL. In *proceeding 5th International conference on the spectroscopy of biological molecules*. Theophanides T, Anastasspoulou J, Fotopoulos N (eds). Kluwer Academis publisher: The Netherlands.
20. Rastogi VK, Lal B, Sharma YC, Jain CL. In *Metal Ions in Biology, Proceedings International Symposium, 2nd*, 1992; 184.
21. Singh R, Tyagi S, Singh S, Singh SM, Singh UP. *Synth. React. Inorg. Met.-Org. Chem.* 2002; **32**: 853.
22. Singh S, Singh R, Babbar P, Singh UP. *Trans. Met. Chem.* 2000; **25**: 9.
23. Fuciarelli AF, Sisk EC, Zimbrick JD. *Int. J. Radiat. Biol.* 1994; **65**: 409.
24. Fuciarelli AF, Sisk EC, Miller JH, Zimbrick JD. *Int. J. Radiat. Biol.* 1994; **66**: 505.
25. Beach C, Fuciarelli AF, Zimbrick JD. *Radiat. Res.* 1994; **137**: 385.
26. Abdoul H-Carime, Huels MA, Bruning F, Illenberger E, Sanche L. *J. Chem. Phys.* 2000; **113**: 2517.
27. Parkanyi C, Boniface C, Aaron JJ, Gaye MD, von Szentpaly L, Ghosh R, RaghuVeer KS. *Struct. Chem.* 1992; **3**(4): 277.
28. Waghorne E, Duggan E, Will G, Fitzmaurice D, Mukherjee S. *Indian J. Phys.* 1999; **73B**: 671.
29. Nagasaka B, Takeda S, Nakamura N. *Chem. Phys. Lett.* 1996; **222**: 486.
30. Rabbani SR, Edmonds DT, Gosling P. *J. Magn. Reson.* 1987; **72**: 422.
31. Sevilla MD, Swarts S, Riederer H, Huttermann J. *J. Phys. Chem.* 1984; **88**: 1601.
32. Rai JN. *Proc. Ind. Acad. Sci. Chem. Sci.* 1990; **102**: 68.
33. Graindourze M, Grootaers T, Smets J, Zeegers-Huyskens Th, Maes G. *J. Mol. Struct.* 1990; **237**: 389.
34. Graindourze M, Grootaers T, Smets J, Zeegers-Huyskens Th, Maes G. *J. Mol. Struct.* 1991; **243**: 37.
35. Gusakova GV, Kul'bida AI, Plekhova GN, Smolyanskii AL. *J. Appl. Spectrosc.* 1987; **46**: 381.
36. Srivastava SL, Prasad Rohitashava M, Pandey VS. *Spectrochim. Acta* 1984; **40A**: 675.
37. Sanyal NK, Srivastava SL, Goel RK. *Indian J. Phys.* 1977; **52 B**: 108.
38. Zwierzchowska Z, Dobrosz-Teperek K, Lewandowski W, Kolos R, Bajdor K, Dobrowolski JCz, Mazurek AP. *J. Mol. Struct.* 1997; **410–411**: 415.
39. Dobrosz-Teperek K, Zwierzchowska Z, Lewandowski W, Bajdor K, Dobrowolski JCZ, Mazurek AP. *J. Mol. Struct.* 1998; **471**: 115.
40. Rastogi VK, Arora S, Gupta SL, Sharma DK. *Spec. Publ. Roy. Soc. Chem.* 1991; **94**: 401, (Spectrosc Biol Mol).
41. Dobrowolski Jan CZ, Rode JE, Kolos R, Jamroz MH, Bajdor K, Mazurek AP. *J. Phys. Chem.* 2005; **109**: 216.
42. Alcolea Palafox M, Iza N, Gil M. *J. Mol. Struct. (THEOCHEM)* 2002; **585**: 69.
43. Del Bene JE. *J. Phys. Chem.* 1982; **86**: 1341.
44. Chandra AK, Uchimaru T, Zeegers-Huyskens T. *J. Mol. Struct.* 2002; **605**: 213.
45. Hehre WJ, Radom L, Schleyer PVR, Pople JA. *Ab Initio Molecular Orbital Theory*. John Wiley and Son: New York, 1986.
46. Pople JA, Krishnan R, Schlegel HB, Binkley JS. *Int. J. Quantum Chem. Quantum Chem. Symp.* 1979; **13**: 225.
47. Seminario JM, Politzer P (eds). *Modern Density Functional Theory; A Tool for Chemistry*, vol 2. Elsevier: Amsterdam, 1995.
48. Becke AD. *Phys. Rev.* 1988; **A 38**: 3098.
49. Becke AD *J. Chem. Phys.* 1992; **97**: 9173.
50. Becke AD *J. Chem. Phys.* 1993; **98**: 5648.
51. Lee C, Yang W, Parr RG. *Phys. Rev.* 1988; **B 37**: 785.
52. Perdew JP. *Phys. Rev.* 1986; **B 33**: 8822.
53. Perdew JP. *Phys. Rev.* 1986; **B 34**: 7406.
54. Perdew JP, Wang Y. *Phys. Rev.* 1992; **B 45**: 13244.
55. Perdew JP, Chevary JA, Vosko SH, Jackson KA, Pederson MR, Singh DJ, Fiolhais C. *Phys. Rev.* 1992; **B46**: 6671.
56. Adamo C, Barone V. *J. Chem. Phys.* 1998; **108**: 664.
57. Woon DE, Dunning TH Jr. *J. Chem. Phys.* 1993; **98**: 1358.
58. Peterson KA, Woon DE, Dunning TH Jr. *J. Chem. Phys.* 1994; **100**: 7410.
59. Wilson A, Van Mourik T, Dunning TH Jr. *J. Mol. Struct. (THEOCHEM)* 1997; **388**: 339.
60. Frisch MJ, Trucks GW, Schlegel HB, Scuseria GE, Robb MA, Cheeseman JR, Zakrzewski VG, Montgomery JA Jr, Stratmann RE, Burant JC, Dapprich S, Millam JM, Daniels AD, Kudin KN, Strain MC, Farkas O, Tomasi J, Barone V, Cossi M, Cammi R, Mennucci B, Pomelli C, Adamo C, Clifford S, Ochterski J, Petersoon GA, Ayala PY, Cui Q, Morokuma K, Malick DK, Rabuck AD, Raghavachari K, Foresman JB, Cioslowski J, Ortiz JV, Baboul AG, Stefanov BB, Liu G, Liashenko A, Piskorz P, Komaromi I, Gomperts R, Martin RL, Fox DJ, Keith T, Al-Laham MA, Peng CY, Nanayakkara A, Challacombe M, Gill PMW, Johnson B, Chen W, Wong MW, Andres JL, Gonzalez C, Head-Gordon M, Replogle ES, Pople JA. *Gaussian 98, Revision A 9*. Gaussian, Inc: Pittsburgh, PA, 1998.
61. Ferenczy G, Harsanyi L, Rozsondai B, Hargittai I. *J. Mol. Struct.* 1986; **140**: 71.
62. Harsanyi L, Csaszar A, Csaszar P. *J. Mol. Struct. (THEOCHEM)* 1986; **137**: 207.
63. Stewart RF, Jensen LH. *Acta Crystallogr.* 1967; **13**: 1102.
64. Aamouche A, Berthier G, Cadioli B, Gallinella E, Ghomi M. *J. Mol. Struct. (THEOCHEM)* 1998; **426**: 307.
65. Williamns RW, Lowrey AH. *J. Comput. Chem.* 1991; **12**: 861.
66. Towasi J, Persico M. *Chem. Rev.* 1994; **94**: 2027.
67. Williams RW, Cheh JL, Lowrey AH, Weif AF. *J. Phys. Chem.* 1995; **99**: 5299.
68. Blicharska B, Kupka T. *J. Mol. Struct.* 2002; **613**: 153.
69. Szczesniak M, Nowak MJ, Szzczepaniak K, Chin S, Scott I, Person WB. *Spectrochim. Acta* 1985; **41A**: 233.
70. Nowak MJ, Lapinski L, Bienko DC, Michalska D. *Spectrochim. Acta* 1997; **53A**: 855.
71. Alcolea Palafox M, Rastogi VK. *Spectrochim. Acta* 2002; **58A**: 411.
72. Roeges NPG. *A Guide to the Complete Interpretation of Infrared Spectra of Organic Structures*. John Wiley and Sons: New York, 1994.
73. Alcolea Palafox M. *Recent. Res. Dev. Phys. Chem.* 1998; **2**.
74. Scott AP, Radom L. *J. Phys. Chem.* 1996; **100**: 16502.
75. Monshi M, Al-Fahan K, Al-Resayes S, Ghaith A, Hasanein AA. *Spectrochim. Acta.* 1997; **53**: 2669.
76. Kulakowska I, Geller M, Lesyng B, Wierzchowski KL. *Biochim. Biophys. Acta* 1947; **361**: 119.

DOI: 10.1002/jrs